Role of the Fas Pathway in *Pseudomonas aeruginosa* Keratitis

Zimei Zhou, Minhao Wu, Ronald P. Barrett, Sharon A. McClellan, Yunfan Zhang, and Linda D. Hazlett

Purpose. The role of the Fas pathway was tested in *Pseudomonas aeruginosa*–infected mouse cornea by contrasting the responses of FasL$^{-/-}$ and wild-type (WT) mice.

Methods. TUNEL staining, real-time RT-PCR, immunostaining, and ELISA assay were used.

Results. Compared with WT (resistant) mice, BALB/c FasL$^{-/-}$ exhibited significantly elevated bacterial counts and polymorphonuclear leukocyte numbers at 1 and 3 days postinfection (p.i.) and worse outcomes from disease. Similar bacterial challenges in C57BL/6 FasL$^{-/-}$ compared with WT mice also led to worsened disease as evidenced by earlier corneal perforation in the susceptible mouse strain. Intense TUNEL staining of apoptotic cells was seen earlier (1 day vs. 3 days) p.i. in BALB/c WT than in knockout mice, This earlier apoptotic pattern correlated with increased expression of caspases 3, 8, and 9 and BAX and with decreased expression of the antiapoptotic molecule Bcl-2. Furthermore, expression levels of the proinflammatory molecule TNF-α and its receptor, MIP-2, inducible nitric oxide synthase (iNOS), and nitrite also were significantly elevated in the infected cornea of BALB/c FasL$^{-/-}$ compared with WT mice. In vitro, LPS-stimulated Mϕ from BALB/c FasL$^{-/-}$ mice expressed significantly less caspase 3 and 9, BAX, and IL-10 and more TNF-α, MIP-2, and IL-1β than did cells from WT mice.

Conclusions. Fas-FasL interaction in the cornea balances the host innate immune response to improve disease outcome by promoting earlier apoptosis and regulating proinflammatory cytokines/chemokines and nitric oxide (nitrite) production. Dysregulation of this interaction contributes to bystander tissue damage, enhancing nutrients for bacterial growth and worsened disease outcome after *P. aeruginosa* infection. (*Invest Ophthalmol Vis Sci.* 2010;51:2537–2547) DOI:10.1167/iovs.09-4152

Infection with *Pseudomonas aeruginosa* is often associated with keratitis, especially in users of extended-wear contact lenses,[1–3] with disease outcome largely determined by the host inflammatory response. In fact, we propose that although an intense response may be needed to eradicate the bacteria, if left uncontrolled, it is often detrimental, favoring bystander tissue damage and in turn providing nutrients for bacterial growth and replication. Thus, tight regulation of inflammation and a balance between proinflammatory and antiinflammatory factors is requisite for disease resolution, including restoration of tissue homeostasis.[4] Whether cells undergo necrosis and when they undergo apoptosis also may contribute to disease outcome. In this regard, previous studies[5] have shown that apoptosis of polymorphonuclear leukocytes (PMNs) is delayed until 3 days p.i. in the corneas of susceptible C57BL/6 (B6) mice, whereas in resistant BALB/c mice, cells undergo apoptosis at 1 day p.i. The importance of earlier apoptosis in disease resolution was further confirmed in B6 mice by blocking interaction of the antiapoptotic neuropeptide substance P with its receptor (NK-1R), which resulted in earlier apoptosis and improved disease outcome.

Apoptosis can be initiated by a variety of interactions, including the interaction between Fas and Fas Ligand (FasL), the well-documented death ligand and its receptor,[6,7] leading to the subsequent activation of downstream caspases and the induction of cell lysis. It has been suggested that the Fas-FasL system may play an important role in the pathophysiology of infectious diseases.[8] Evidence shows that *P. aeruginosa* infection induces lung epithelial cell apoptosis through the activation of endogenous Fas and FasL in vitro and in vivo, leading to improved disease outcomes in C3H mice.[8] Others have reported that ExoS of *P. aeruginosa* triggers apoptosis in various cultured cell lines through clustering membrane Fas and activating the Fas-FasL pathway.[9] Evidence has also suggested a direct regulatory role of the Fas-FasL system on local cytokine/chemokine production.[10] For example, it was reported that C3H/HeJ^{gld} mice, which bear a nonfunctional mutation in FasL, showed significantly reduced *Borrelia burgdorferi*–specific cytokine response and reduced severity of arthritis.[10] However, whether Fas-FasL interaction functions in *P. aeruginosa*–induced keratitis and has a similar impact on disease outcome remain to be determined.

Our studies provide evidence that compared with WT mice, FasL$^{-/-}$ mice have a delayed onset of apoptosis and an exacerbated production of proinflammatory cytokines/chemokines and nitric oxide (NO) after *P. aeruginosa* corneal challenge, subsequently leading to worsening of disease. We also document in vitro that LPS-stimulated Mϕ from FasL$^{-/-}$ mice compared with WT BALB/c mice showed decreased apoptosis, increased production of TNF-α, MIP-2, and IL-1β, and decreased production of IL-10, consistent with our in vivo findings.

Methods

Mice

Female 7- to 8-week-old CPt.C3-Fasl^{gld}/J (BALB/c FasL$^{-/-}$), B6Smn.C3-Fasl/J (B6 FasL$^{-/-}$), BALB/cJ (BALB/c wt), and C57BL/6/J (B6 wt) mice were purchased from the Jackson Laboratory (Bar Harbor, ME) and housed according to the National Institutes of Health guidelines. All procedures conformed to the ARVO Statement for the Use of Animals in Ophthalmic and Vision Research.

From the Department of Anatomy and Cell Biology, Wayne State University School of Medicine, Detroit, Michigan.

Supported by National Institutes of Health Grants R01 EY02986, EY016058, and P30 EY04068.

Submitted for publication June 16, 2009; revised October 2, 2009; accepted November 15, 2009.

Disclosure: **Z. Zhou**, None; **M. Wu**, None; **R.P. Barrett**, None; **S.A. McClellan**, None; **Y. Zhang**, None; **L.D. Hazlett**, None

Corresponding author: Linda D. Hazlett, Department of Anatomy and Cell Biology, 540 East Canfield Avenue, Detroit, MI 48201; lhazlett@med.wayne.edu.

Bacterial Infection and Ocular Response

P. aeruginosa strain 19660 was purchased from the American Type Culture Collection (ATCC, Manassas, VA), and cultures were prepared as described.[11] For infection, mice were anesthetized with ethyl ether, the left central cornea was scarified with a 25-gauge needle, and a 5-μL aliquot containing a 1×10^6 CFU/μL bacterial suspension applied. Disease was graded at 1, 3, and 5 days p.i. using an established scale.[11,12]

Quantitation of Viable Bacteria

Bacteria were quantitated at 1 and 3 days p.i. in individual infected corneas of FasL$^{-/-}$ and WT mice (n = 5/group/time).[13,14] Each cornea was homogenized in 1 mL sterile saline containing 0.25% BSA, and the homogenate (0.1 mL) was serially diluted 1:10 in the same solution. Selected dilutions were plated in triplicate on *Pseudomonas* isolation agar (Difco, Detroit, MI) and, incubated overnight at 37°C, and viable bacteria were counted. Results are reported as 10^5 CFU/cornea ± SEM.

Quantitation of PMN

Myeloperoxidase (MPO) assay was used to quantitate PMNs in the corneas of FasL$^{-/-}$ compared with WT mice (n = 5/group/time) at 1 and 3 days p.i.[15,16] Corneas were removed and homogenized in 1 mL of 50 mM phosphate buffer (pH 6.0) containing 0.5% HTAB (Sigma-Aldrich, St. Louis, MO), freeze-thawed four times, and centrifuged, and 0.1 mL was added to 2.9 mL of 50 mM phosphate buffer containing *o*-dianisidine dihydrochloride (16.7 mg/100 mL) and 0.0005% hydrogen peroxide. Change in absorbance at 460 nm was read on a spectrophotometer (Helios; Thermo Spectronic, Pittsford, NY), and units of MPO/cornea were calculated. One unit of MPO activity is equivalent to $\sim 2 \times 10^5$ PMN/mL.[17,18]

Griess Reaction

NO levels were determined by measuring its stable end product, nitrite, using a Griess reagent (1% sulfanilamide/0.1% naphthyl ethylene diamine dihydrochloride 12.5% H_3PO_4; Sigma-Aldrich) for BALB/c FasL$^{-/-}$ compared with WT mice (n = 5/group/time).[4,19] Infected corneas were homogenized in 500 μL degassed PBS and microcentrifuged at 3500 rpm (5 minutes). Next, 100 μL supernatant was added to an equal volume of Griess reagent in duplicate on a 96-well microtiter plate and incubated at room temperature (15 minutes). Absorbance (540 nm) was measured, and nitrite concentrations were estimated using a standard curve of sodium nitrite. Data are represented as the mean micromoles of nitrite per cornea ± SEM.

Mϕ Isolation and Stimulation Assay

Peritoneal Mϕ were elicited and isolated from BALB/c FasL$^{-/-}$ and WT mice as described.[4,5] To induce Mϕ into the peritoneal cavity, 1 mL of 3% Brewer's thioglycollate medium (Difco) was injected intraperitoneally 5 days before harvesting. Cells were collected by peritoneal lavage and stained by trypan blue, and viable cells (>95%) were counted with a hemacytometer. Mϕ were seeded in 12-well plates at a density of 1×10^6 cells/well, and nonadherent cells were removed 4 hours later. Isolated Mϕ were stimulated with *P. aeruginosa* LPS serotype 10 (Sigma; 100 ng/mL, 1 μg/mL, 10 μg/mL, and 25 μg/mL) for 18 hours. Cells were collected; mRNA was extracted and assayed by real-time RT-PCR for selected cytokines/chemokines and apoptosis-related genes. The supernatant from each well was collected and assayed by ELISA for selected cytokines/chemokines.

TUNEL Assay

Normal uninfected and infected BALB/c FasL$^{-/-}$ and WT mouse eyes (n = 3/group/time) were enucleated at 1 and 3 days p.i. for TUNEL staining with a terminal deoxynucleotidyl transferase (TdT) kit (TACS; R&D Systems, Minneapolis MN) according to the manufacturer's instructions.[5] Eyes were fixed in a 3.7% formaldehyde solution and embedded in paraffin. Ten micrometer–thick sections were cut, deparaffinized, rehydrated, and rinsed with DNase-free water. Sections were permeabilized using proteinase K solution (15 minutes), followed by quenching of endogenous peroxidase using 3% H_2O_2 in methanol (5 minutes). Sections were incubated with 1× TdT enzyme solution (1 hour) at 37°C in a humidity chamber to label DNA nick ends, and the reaction was stopped with TdT stop buffer (5 minutes). Color was developed using streptavidin-HRP detection solution (10 minutes) followed by incubation with TdT blue label solution (5 minutes) and counterstaining with nuclear fast red (5 minutes). All procedures were conducted at room temperature, unless indicated. Control samples were treated similarly but without TdT enzyme. Sections were photographed under a microscope (Axiophot; Carl Zeiss, Oberkochen, Germany) with digital imagery (Axiocam; Carl Zeiss).

TUNEL and PMN Immunostaining

Infected BALB/c FasL$^{-/-}$ mouse eyes (n = 5) were enucleated at 3 days p.i., fixed, embedded, and sectioned. Alternate serial sections were stained for TUNEL, as described, or PMN by specific immunostaining. For PMN staining, sections were rehydrated and blocked with rabbit IgG (1:100; Sigma-Aldrich) diluted in 0.01 M phosphate buffer containing 2.5% BSA for 30 minutes. Sections were then incubated with a primary rat anti-PMN–specific antibody NIMP-R14 (1:80; Abcam, Cambridge, MA), followed by incubation with a biotinylated secondary rabbit anti–rat IgG antibody (1:1000; Vector Laboratories, Burlingame, CA) for 1 hour each and then incubated (30 minutes) with peroxidase-conjugated extravidin for color development. Control sections were similarly processed, omitting the primary antibody. In TUNEL and PMN staining, sections were counterstained (Fast Green; 1:100; Fisher Scientific, Pittsburgh, PA). Sections were photographed under a microscope (Axiophot; Zeiss) as described.

Immunofluorescence Staining and Confocal Microscopy

Normal uninfected and infected eyes from BALB/c FasL$^{-/-}$ and WT mice (n = 3/group/time) were enucleated at 1 day p.i. Eyes were immersed in optimal cutting temperature (Tissue Tek; Miles, Elkhart, IN), frozen in liquid nitrogen, sectioned at 10 μm, and collected onto polylysine-coated glass slides. Nonspecific staining for activated caspase 3[5] and Bcl-2[20] was blocked using goat or donkey IgG, respectively (each at 1:100; Molecular Probes, Eugene, OR) diluted in 0.01 M phosphate buffer containing 2.5% BSA for 30 minutes. Slides then were incubated with primary rabbit anti–mouse cleaved caspase 3 (Asp 175) antibody (1:200; Cell Signaling Technology, Danvers, MA) or primary rabbit anti-rat/mouse Bcl-2 polyclonal antibody (1:800; BD PharMingen, San Diego, CA) for 1 hour. Slides were then incubated for 1 hour with secondary Alexa Fluor 633 goat anti-rabbit IgG (1:1500; Molecular Probes) for caspase 3 or secondary Alexa Fluor 594 donkey anti–rabbit antibody (1:1500; Molecular Probes) for Bcl-2. Slides were incubated for 2 minutes using nuclear acid stain (1:10,000; SYTOX Green; Lonza, Walkersville, MD). Negative controls were similarly treated, but primary antibodies were replaced with rabbit IgG (1:200 or 1:800; Molecular Probes). All procedures were at room temperature unless indicated. Sections were visualized, and digital images were captured with a confocal laser scanning microscope (TSC SP2; Leica Microsystems, Bannockburn, IL).

Real-time RT-PCR

Normal uninfected and infected corneas from BALB/c, B6 FasL$^{-/-}$, and WT mice (n = 5/group/time) were removed at 1, 3, and 5 days p.i. and were stored at −20°C (RNAlater; Ambion Inc., Austin, TX) for real-time RT-PCR analysis.[5] In separate experiments, isolated Mϕ were collected from BALB/c FasL$^{-/-}$ and WT mice as described. For both, total RNA was extracted with reagent (RNA STAT-60; Tel-Test, Friendsville, TX) according to the manufacturer's instruction, precipitated using isopropanol (0.5 mL/1 mL RNA STAT-60; Tel-Test), and washed with 75% ethanol. One microgram of each RNA sample was reverse transcribed (M-MLV Reverse Transcriptase; Invitrogen, Carlsbad, CA) in a 20-μL volume. cDNA products were diluted 1:10 with diethylpyrocarbonate-treated H_2O and 2 μL of each cDNA dilution used for real-time RT-PCR.

TABLE 1. Nucleotide Sequences of the Specific Primers Used in PCR Amplification

Gene	Primer Sequence	Sense
β-Actin	5′-GAT TAC TGC TCT GGC TCC TAG C-3′	F
	5′-GAC TCA TCG TAC TCC TGC TTG C-3′	R
Caspase 3	5′-TGG GCC TGA AAT ACC AAG TC-3′	F
	5′-AAA TGACCC CTT CAT CAC CA-3′	R
Caspase 9	5′-GCC AGA GGT TCT CAG ACC AG-3′	F
	5′-TCC CTG GAA CAC AGA CAT CA-3′	R
BAX	5′-CGA GCT GAT CAG AAC CAT CA-3′	F
	5′-CTC AGC CCA TCT TCT TCC AG-3′	R
Bcl-2	5′-GGA CTT GAA GTG CCA TTG GT-3′	F
	5′-AGC CCC TCT GTG ACA GCT TA-3′	R
Caspase 8	5′-GGC CTC CAT CTA TGA CCT GA-3′	F
	5′-GTG TGG TTC TGT TGC TCG AA-3′	R
Tnfrsf12a	5′-CAG ATC CTC GTG TTG GGA TT-3′	F
	5′-CAG TCC ATG CAC TTG TCG AG-3′	R
iNOS	5′-TCC TCA CTG GGA CAG CAC AGA ATG-3′	F
	5′-GTG TCA TGC AAA ATC TCT CCA CTG CC-3′	R
IL-12	5′-GGT CAC ACT GGA CCA AAG GGA CTA TG-3′	F
	5′-ATT CTG CTG CCG TGC TTC CAA C-3′	R
MIP-2	5′-TGT CAA TGC CTG AAG ACC CTG CC-3′	F
	5′-AAC TTT TTG ACC GCC CTT GAG AGT GG-3′	R
IL-1β	5′-CGC AGC AGC ACA TCA ACA AGA GC-3′	F
	5′-TGT CCT CAT CCT GGA AGG TCC ACG-3′	R
IL-10	5′-TGC TAA CCG ACT CCT TAA TGC AGG AC-3′	F
	5′-CCT TGA TTT CTG GGC CAT GCT TCT C-3′	R
TNF-α	5′-ACC CTC ACA CTC AGA TCA TCTT-3′	F
	5′-GGT-TGT CTT TGA GAT CCA TGC-3′	R

F, forward; R, reverse.

Real-time RT-PCR was performed with an RT-PCR detection system (MyiQ Single Color Real-time; Bio-Rad, Hercules, CA). Supermix (iQ SYBR Green; Bio-Rad) was used for each PCR reaction with a primer concentration of 5 μM. PCR parameters used were preheating at 95°C for 3 minutes followed by 45 cycles of amplification (15 seconds at 95°C and 40 seconds at 60°C). Primer pair sequences are shown in Table 1. mRNA fold changes were calculated after normalization to β-actin.

ELISA

MIP-2 protein levels were determined in BALB/c FasL$^{-/-}$ compared with WT mice by ELISA (R&D Systems). Corneas from infected mice (n = 5/group/time) were harvested at 1 and 3 days p.i., individually homogenized in PBS containing 0.1% Tween-20 and protease inhibitors (Roche, Indianapolis, IN) using a glass microtissue grinder, and centrifuged at 13,000 rpm for 10 minutes. Supernatants were diluted 1:50, and 50 μL was used for MIP-2 assay. In another experiment, peritoneal Mϕ were harvested from BALB/c FasL$^{-/-}$ compared with WT mice and were stimulated using LPS at various concentrations, as described. Undiluted sample supernatant (50 μL) was used to assay for TNF-α protein levels using an ELISA kit (R&D Systems). The reported sensitivity of these assays was <1.5 pg/mL for MIP-2 and <5.1 pg/mL for TNF-α.

Statistical Analysis

Differences in clinical scores between BALB/c and B6 FasL$^{-/-}$ and their corresponding WT mice were analyzed by the Mann-Whitney U test. For bacterial counts, MPO, Griess reaction, real-time RT-PCR, and ELISA data, an unpaired, two-tailed Student's t-test was used to determine statistical significance. All experiments were performed twice. Data from both experiments are shown unless otherwise indicated; data were considered significant at $P < 0.05$.

RESULTS

Disease Response, Bacterial Load, and PMN Infiltration

After corneal infection (Fig. 1A), more severe disease was noted in BALB/c FasL$^{-/-}$ than in WT mice at 3 and 5 days p.i. ($P < 0.0001$ for each) but not at 1 day p.i. ($P = 0.28$). Two of 10 eyes were perforated at 5 days p.i. in BALB/c FasL$^{-/-}$, but none were perforated in WT mice. Photomicrographs taken with a slit lamp at 5 days p.i. revealed slight opacity fully covering the cornea in BALB/c WT mice, graded as a clinical score of +1 (Fig. 1B). In contrast, dense opacity covering the anterior segment (clinical score of +3) was seen in BALB/c FasL$^{-/-}$ mice (Fig. 1C). Bacterial load in the BALB/c FasL$^{-/-}$ mouse cornea (Fig. 1D) was significantly higher at 1 and 3 days p.i. ($P < 0.001$ for both) than in WT mice. An MPO assay tested whether Fas-FasL interaction also had an effect on PMN infiltration/persistence in the infected cornea (Fig. 1E) and revealed that the corneas of BALB/c FasL$^{-/-}$ mice contained significantly more PMN than did those of WT mice at both 1 and 3 days p.i. ($P = 0.03$ and $P = 0.01$, respectively).

Similarly, we tested disease response in B6 FasL$^{-/-}$ compared with WT mice. These mice (Fig. 2A) showed earlier perforation than WT controls. At 3 days p.i., 7 of 10 eyes perforated in the FasL$^{-/-}$ group compared with only 1 of 10 in the WT group ($P = 0.04$). Photomicrographs taken with a slit lamp at 3 days p.i. confirmed more severe disease response in B6 FasL$^{-/-}$ compared with WT mice. Dense opacity covering the anterior segment was seen in WT mice (Fig. 2B) compared with severe corneal thinning/perforation in FasL$^{-/-}$ mice (Fig. 2C). Corneal bacterial load in B6 FasL$^{-/-}$ compared with WT mice (Fig. 2D) was significantly higher at 1 and 3 days p.i. ($P < 0.001$ for both). MPO assay (Fig. 2E) showed that corneas of B6 FasL$^{-/-}$ mice contained significantly more PMNs than did corneas of WT mice (1 and 3 days p.i.; $P < 0.001$ for both).

TUNEL Staining

Apoptosis in the infected corneas of BALB/c FasL$^{-/-}$ compared with WT mice was assessed by TUNEL staining (Figs. 3A–D). At 1 day p.i., the corneas of BALB/c WT mice (Fig. 3A) showed more intense TUNEL-positive staining than did corneas of BALB/c FasL$^{-/-}$ mice (Fig. 3C). In the latter, apoptosis was delayed until 3 days p.i. (Fig. 3D) and was more intense at that time than staining in WT mice (Fig. 3B). No TUNEL staining was detected in normal, uninfected corneas or in control sec-

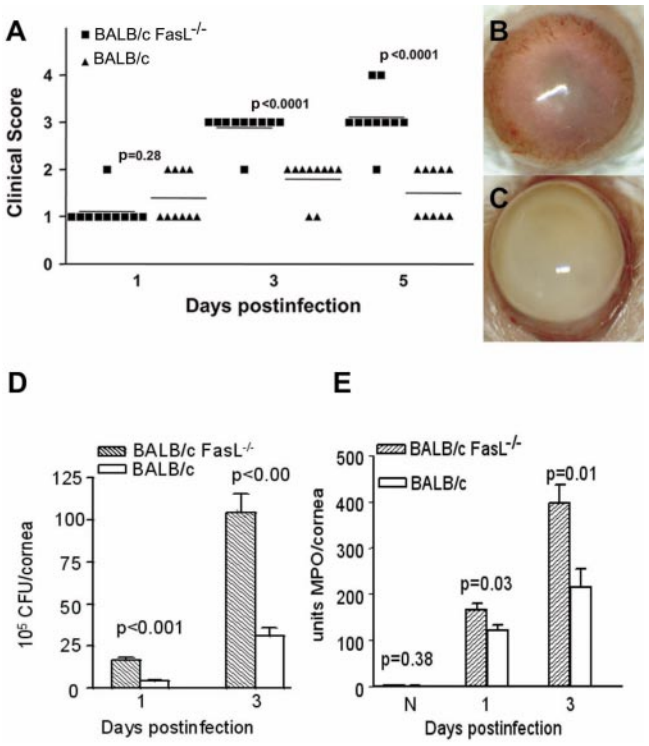

FIGURE 1. Disease in BALB/c FasL$^{-/-}$ compared with WT mice. (**A**) Corneal disease was graded at 1, 3, and 5 days p.i. (n = 5/group/time). BALB/c FasL$^{-/-}$ compared with WT mice had worsened disease at 3 and 5 days p.i. ($P < 0.0001$). (**B**, **C**) Photographs taken with a slit lamp. Eyes from BALB/c WT (**B**) and FasL$^{-/-}$ mice (**C**) are shown at 5 days p.i. Original magnification, 15×. (**D**) Viable bacterial plate counts. BALB/c FasL$^{-/-}$ compared with WT mice (n = 5/group/time) had significantly more bacteria at 1 and 3 days p.i. ($P < 0.001$). Results are reported as 10^5 CFU/cornea ± SEM. (**E**) PMNs per cornea (mean ± SEM; n = 5/group/time) determined by MPO assay. More PMNs were detected in the corneas of BALB/c FasL$^{-/-}$ than WT mice at 1 (P = 0.03) and 3 (P = 0.01) days p.i.

tions in the absence of the TdT enzyme in either group (data not shown).

Real-time RT-PCR

Caspases 3 (Fig. 3E; effector caspase) and 9 (Fig. 3F; initiator caspase) mRNA expression was increased at 1 day p.i. in BALB/c WT than in FasL$^{-/-}$ mouse corneas (P = 0.01 and P = 0.03 respectively), whereas at 3 days p.i., the corneas of BALB/c FasL$^{-/-}$ compared with WT mice expressed more mRNA for these two caspases ($P < 0.001$ for both). At 5 days p.i., mRNA levels of caspase 9 remained upregulated in BALB/c FasL$^{-/-}$ compared with WT mouse corneas ($P < 0.001$), but no difference between groups was detected for caspase 3. Caspase 8 (Fig. 3G; initiator caspase) expression was decreased at 1, 3, and 5 days p.i. in BALB/c FasL$^{-/-}$ compared with WT mouse corneas (P = 0.001, $P < 0.001$ and P = 0.001, respectively). mRNA levels for BAX (Fig. 3H; proapoptotic regulator) was significantly lower in the corneas of BALB/c FasL$^{-/-}$ than of WT mice at 1 day p.i. (P = 0.004) but not at 3 and 5 days p.i. Bcl-2 (Fig. 3I; antiapoptosis gene) was elevated in the corneas of BALB/c FasL$^{-/-}$ mice at 1 day p.i. (P = 0.002) but was downregulated at 3 and 5 days p.i. (P = 0.03, $P < 0.001$, respectively) compared with WT mice. Apoptosis-related gene expression also was selectively tested in infected B6 FasL$^{-/-}$ mice compared with WT mice. Caspase 3 (Fig. 3J) mRNA expression was increased at 3 days p.i. in B6 WT versus FasL$^{-/-}$ mouse corneas (P = 0.008). No significant difference between groups was detected at 1 day or 5 days p.i. mRNA levels for BAX (Fig. 3K) were significantly higher in the corneas of B6 WT versus FasL$^{-/-}$ mice at 1 day and 3 days p.i. (P = 0.001 and P = 0.03, respectively) but not 5 days p.i. mRNA for Bcl-2 (Fig. 3L) was elevated in the corneas of B6 FasL$^{-/-}$ mice at 3 days p.i. ($P < 0.001$), but not at 1 and 5 days p.i. when compared with WT mice. No difference in expression was detected in the normal, uninfected cornea between groups for the genes tested.

Immunofluorescence Staining and Confocal Microscopy

Caspase 3 and Bcl-2 mRNA expression in BALB/c WT versus FasL$^{-/-}$ mice was confirmed by immunostaining and confocal laser scanning microscopy (Figs. 4 and 5). Activated caspase 3-specific staining (Figs. 4A–F, red) was more intense at 1 day p.i. in the corneal stroma of WT (Fig. 4A) versus FasL$^{-/-}$ (Fig. 4B) mice. At 3 days p.i., stromal staining for caspase 3 was greater in FasL$^{-/-}$ (Fig. 4E) than in WT (Fig. 4B) mice. Control sections (rabbit IgG instead of primary antibodies) showed nonspecific staining for caspase 3 in the corneal epithelium but none in the stroma (Figs. 4C, 4F) for both groups. Specific Bcl-2 staining (Figs. 5A–F, red) was more intense in the cornea at 1 day p.i. in FasL$^{-/-}$ (Figs. 5B, 5D) than in WT (Figs. 5C, 5D) mice. For Bcl-2, no detectable nonspecific staining was seen in control sections

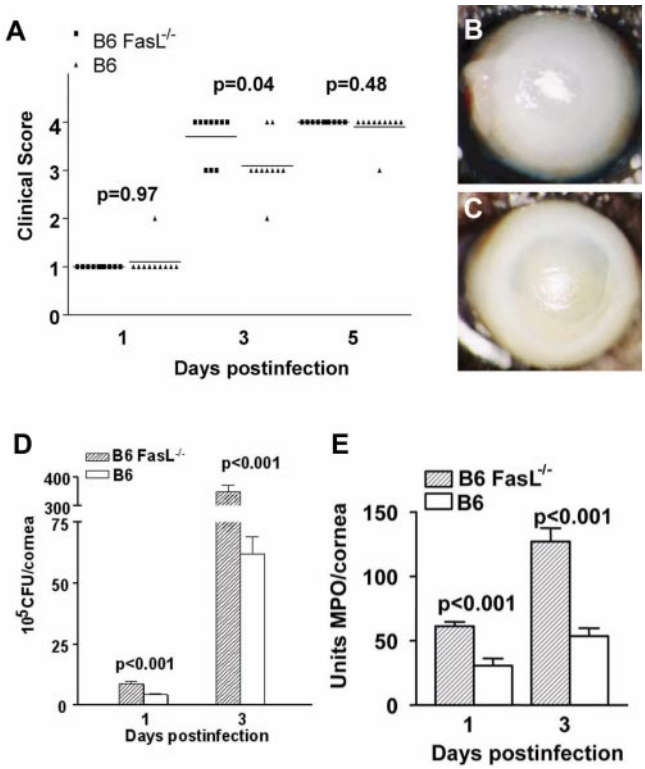

FIGURE 2. Disease in B6 FasL$^{-/-}$ compared with B6 WT mice. (**A**) Corneal disease was graded at 1, 3, and 5 days p.i. (n = 5/group/time). Differences between the groups were seen at 3 days p.i. (P = 0.04). Seven of 10 corneas in B6 FasL$^{-/-}$ compared with 2 of 10 in WT mice perforated by 3 days p.i. No difference was detected between the groups at 5 days p.i. (**B**, **C**) Photomicrographs taken with a slit lamp. Eyes from B6 WT (**B**) and B6 FasL$^{-/-}$ mice (**C**) are shown at 3 days p.i. Original magnification, 15×. (**D**) Viable bacterial plate counts. B6 FasL$^{-/-}$ compared with WT mice (n = 5/group/time) had more bacteria at 1 and 3 days p.i. ($P < 0.001$). Results are reported as 10^5 CFU/cornea ± SEM. (**E**) PMNs per cornea (mean ± SEM; n = 5/group/time) determined by MPO assay. More PMNs were detected in the corneas of B6 FasL$^{-/-}$ than in WT mice at 1 and 3 days p.i. ($P < 0.001$).

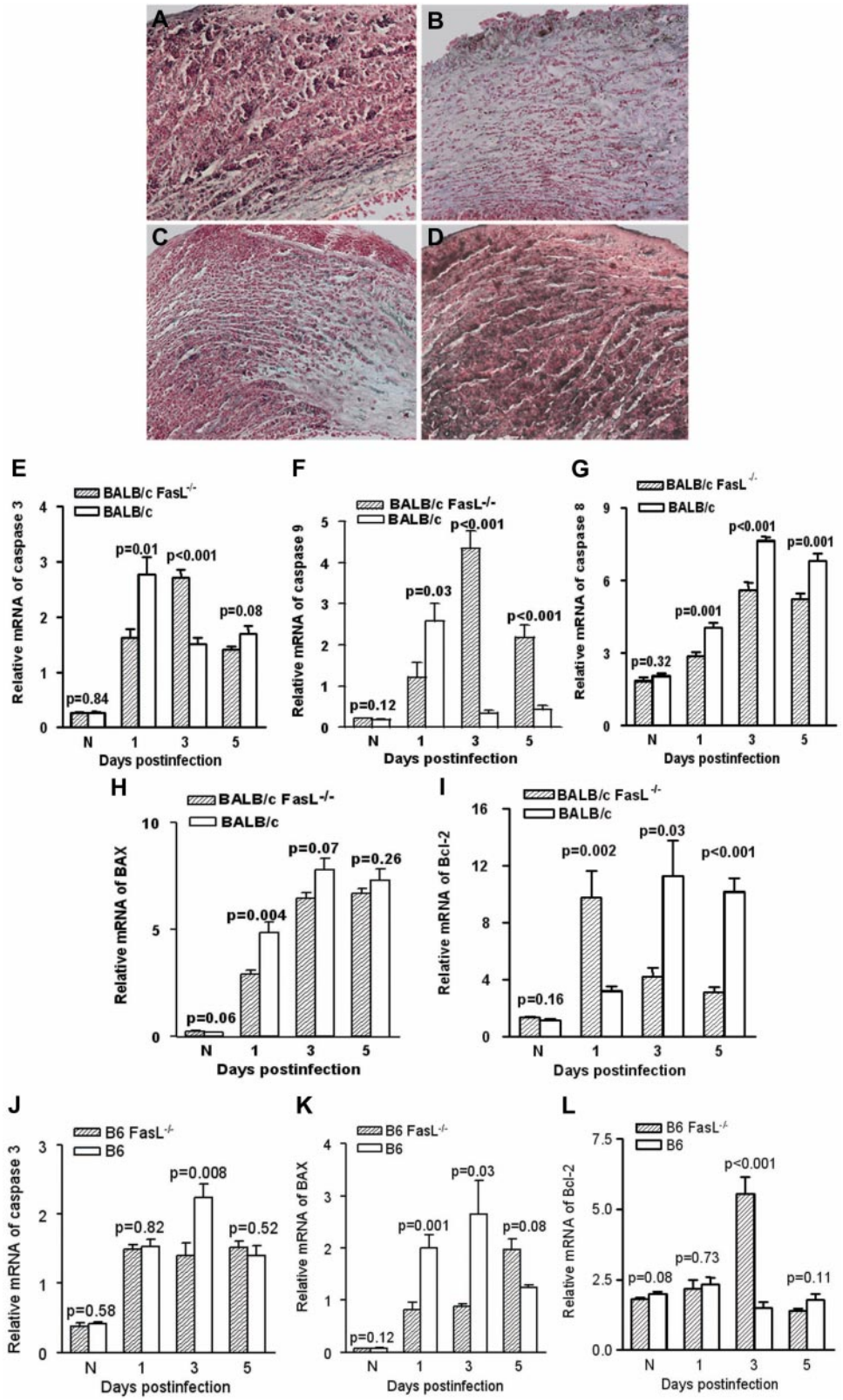

FIGURE 3. Apoptosis in the infected cornea. (**A–D**) Early (1 day p.i.), intense TUNEL-positive staining was detected in the paracentral corneas of BALB/c WT (**A**) than in BALB/c FasL$^{-/-}$ (**C**) mice. At 3 days p.i., BALB/c FasL$^{-/-}$ (**D**) compared with WT (**B**) corneas had greater TUNEL staining. Original magnification, 75× (n = 3/group/time/test). (**E–L**) Real-time RT-PCR of apoptosis-related genes (n = 5/group/time/test). (**E**) mRNA expression levels for caspase 3 were lower at 1 day ($P = 0.01$) but higher at 3 days ($P < 0.001$) p.i. in BALB/c FasL$^{-/-}$ than in WT mouse corneas. No difference was detected at 5 days p.i. between groups. (**F**) Caspase 9 mRNA levels were lower at 1 day ($P = 0.03$) but higher at 3 ($P < 0.001$) and 5 ($P < 0.001$) days p.i. in BALB/c FasL$^{-/-}$ than WT mouse corneas. (**G**) Caspase 8 mRNA levels were downregulated at 1 ($P = 0.001$), 3 ($P < 0.001$), and 5 ($P = 0.001$) days p.i. in BALB/c FasL$^{-/-}$ than in WT mice. (**H**) mRNA levels for BAX were upregulated at 1 day p.i. in BALB/c WT compared with FasL$^{-/-}$ mice ($P = 0.004$). No differences were detected between groups at 3 and 5 days p.i. (**I**) Corneal Bcl-2 expression was upregulated at 1 day ($P = 0.002$) but downregulated at 3 ($P = 0.03$) and 5 ($P < 0.001$) days p.i. in BALB/c FasL$^{-/-}$ compared with WT mice. (**J**) Caspase mRNA expression was increased at 3 days p.i. in B6 WT versus FasL$^{-/-}$ mouse cornea ($P = 0.008$). No difference was detected at 1 or 5 days p.i. between groups. (**K**) Corneal mRNA levels for BAX were upregulated at 1 day ($P = 0.001$) and 3 days ($P = 0.03$) p.i. in B6 WT versus FasL$^{-/-}$ mice. No difference was detected between groups at 5 days p.i. (**L**) Corneal Bcl-2 expression was upregulated at 3 days p.i. in B6 FasL$^{-/-}$ compared with WT mice ($P < 0.001$). No difference was detected at 1 or 5 days p.i. or in normal, uninfected corneas between groups for either of the genes tested.

(IgG substituted for primary antibody), which appeared similar to SYTOX green–stained sections (Figs. 5E, 5F).

TUNEL and PMN Staining

Sequential sections (Fig. 6) confirmed that, in the absence of FasL, many PMN (Fig. 6A) were TUNEL (Fig. 6B) positive in BALB/c FasL$^{-/-}$ mice at 3 days p.i. No positive staining was detected when the TdT enzyme was omitted for TUNEL or the primary antibody for PMN staining (data not shown).

Real-time RT-PCR and ELISA

Real-time RT-PCR and ELISA assays tested the effects of Fas-FasL interaction on proinflammatory cytokine/chemokine production in the infected BALB/c mouse cornea (Figs. 7A–D). No

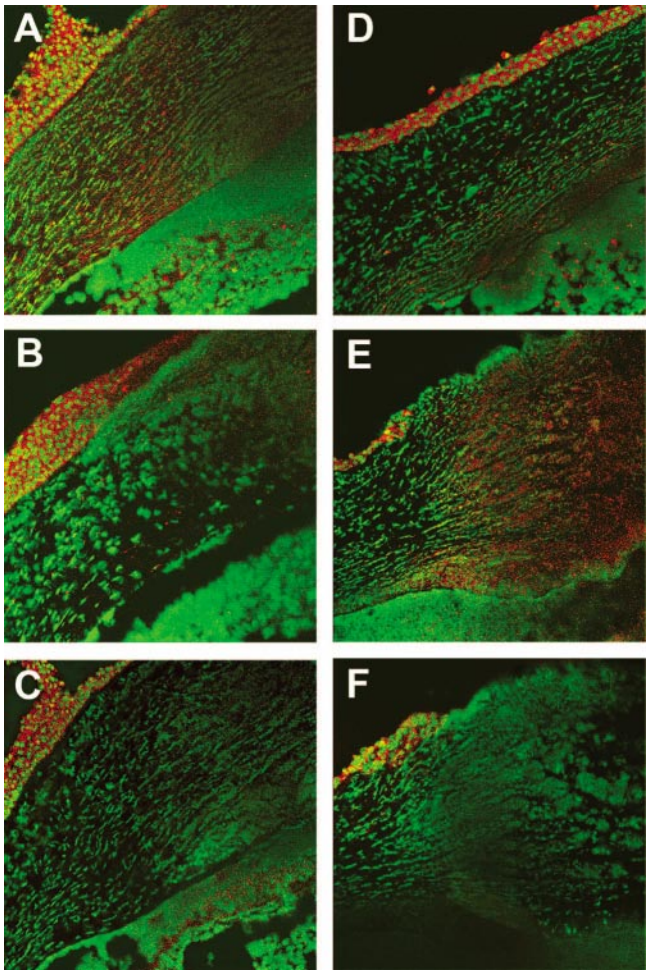

FIGURE 4. Corneal immunostaining for activated caspase 3 (**A–F**) in infected BALB/c FasL$^{-/-}$ (**B**, **E**) compared with WT (**A**, **D**) mice at 1 day (**B**, **A**) and 3 days (**E**, **D**) p.i. (n = 3/group/time/test). More intense activated specific caspase 3 staining (*red*) was detected in WT versus FasL$^{-/-}$ at 1 day p.i. but was delayed in FasL$^{-/-}$ mouse corneal stroma until 3 days p.i. Substitution of the primary antibody with rabbit IgG showed nonspecific staining (**C**, **F**, *red*) in the corneal epithelium but not in the stroma. Original magnification, 45×.

difference in mRNA expression levels for TNF-α (Fig. 7A) or Tnfrsf12a (TNF-α receptor; Fig. 7B) was detected at 1 day p.i. in BALB/c FasL$^{-/-}$ compared with WT mice; however, at 3 ($P = 0.04$ and $P = 0.05$) and 5 ($P < 0.001$ for each) days p.i., BALB/c FasL$^{-/-}$ mice showed higher TNF-α and receptor mRNA levels than did WT mice. MIP-2 expression levels were significantly upregulated at 1 ($P = 0.03$) day p.i. for mRNA (Fig. 7C) and protein ($P < 0.001$) (Fig. 7D) in BALB/c FasL$^{-/-}$ compared with WT mice. At 3 days p.i., BALB/c FasL$^{-/-}$ mice showed slightly, though not significantly, increased MIP-2 mRNA levels than did WT mice ($P = 0.25$) but significantly increased MIP-2 protein levels ($P < 0.001$). No difference was detected at 5 days p.i. for MIP-2 mRNA expression between the groups.

iNOS mRNA and Nitrite Levels

Elevated mRNA expression of iNOS (Fig. 7E) at 3 and 5 days p.i. in the BALB/c FasL$^{-/-}$ compared with the WT mouse cornea ($P < 0.001$ for both) was detected. No difference between the two groups occurred at 1 day p.i. BALB/c FasL$^{-/-}$ compared with WT mice showed increased corneal levels of nitrite at 3 days ($P < 0.001$), but not 1 day, p.i. (Fig. 7F)

Real-time RT-PCR of LPS-Stimulated Mϕ

Mϕ are important cells in bacterial keratitis.[5,21] Thus, we tested their regulation by the Fas pathway in vitro. When comparing LPS-stimulated Mϕ from BALB/c FasL$^{-/-}$ compared with WT mice, mRNA expression for caspase 3 (Fig. 8A) was significantly decreased at concentrations of 100 ng/mL and of 1 and 10 μg/mL ($P = 0.01$, $P < 0.001$, and $P = 0.003$, respectively). No difference was detected at 25 μg/mL or after PBS treatment between the two groups. Caspase 9 (Fig. 8B) mRNA levels were significantly lower at LPS concentrations of 1, 10, and 25 μg/mL ($P = 0.03$ for all) in Mϕ from BALB/c FasL$^{-/-}$ compared with WT mice, but not different at 100 ng/mL or after PBS treatment. mRNA expression of BAX (Fig. 8C) was decreased at LPS concentrations of 10 and 25 μg/mL ($P = 0.008$ and $P < 0.001$, respectively) in cells of BALB/c FasL$^{-/-}$ compared with WT mice but was not different at 100 ng/mL or 1 μg/mL or after PBS treatment.

Real-time RT-PCR and ELISA for Cytokines/Chemokines

Mϕ from BALB/c FasL$^{-/-}$ compared with WT mice expressed more TNF-α mRNA (Fig. 8A) at LPS concentrations of 1 and 10 μg/mL ($P = 0.04$ and $P = 0.03$, respectively). No difference

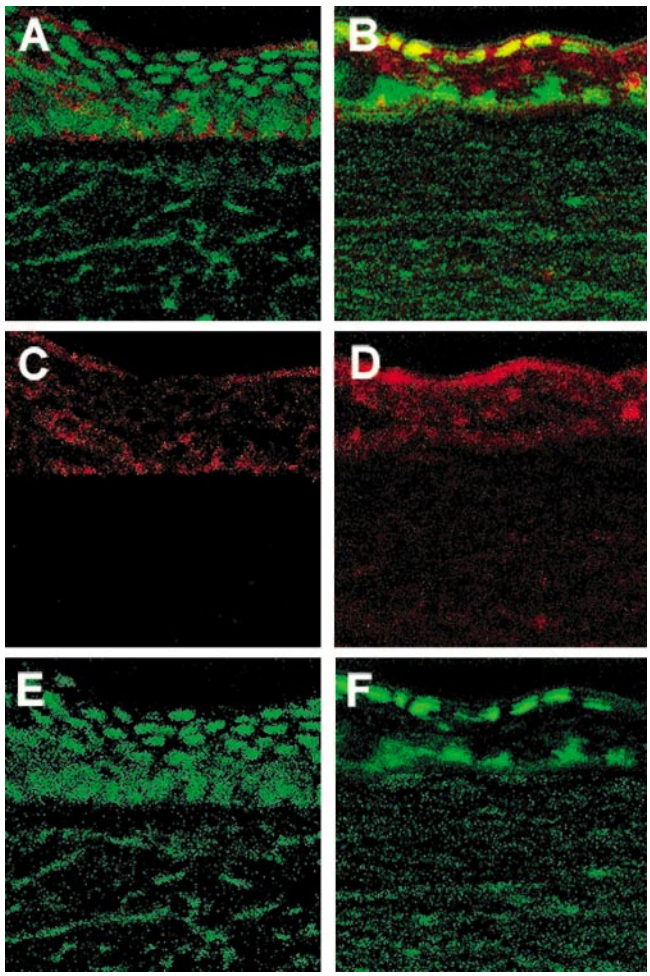

FIGURE 5. Immunostaining for Bcl-2 in the infected BALB/c FasL$^{-/-}$ (**B**, **D**, **F**) compared with WT (**A**, **C**, **E**) cornea at 1 day p.i. (n = 3/group/time/test). More intense Bcl-2 staining (*red*) was detected in FasL$^{-/-}$ compared with WT mouse corneal epithelium (*top*, merged image; *middle*, Bcl-2 staining alone). SYTOX green nuclear label (**E**, **F**) appeared similar to substitution of the primary antibody with rabbit IgG. Original magnification, 280×.

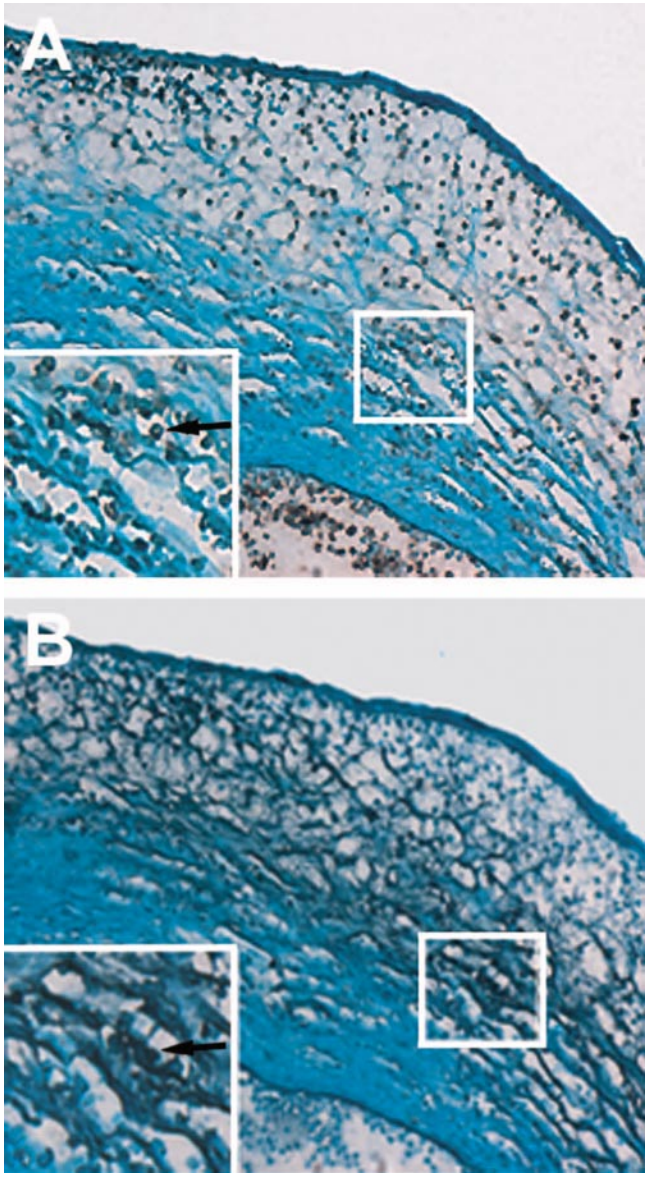

FIGURE 6. TUNEL and PMN staining. PMN (**A**) and TUNEL labeling (**B**) were detected in BALB/c FasL$^{-/-}$ mice at 3 days p.i. *Insets*: magnified images of corresponding regions in two sequential serial sections. At this time, most PMNs in BALB/c FasL$^{-/-}$ mouse corneas were TUNEL positive (*black arrows*). Negative controls, omitting TdT enzyme or primary anti-PMN antibody, showed no positive staining (data not shown). Magnifications: 75× (low magnification); 180× (large inset).

between the two groups was detected after PBS treatment or at LPS concentrations of 100 ng/mL or 25 μg/mL. TNF-α protein levels (Fig. 9B) were increased in supernatants of BALB/c FasL$^{-/-}$ compared with WT Mϕ at all LPS concentrations tested compared with PBS treatment ($P < 0.001$, $P < 0.001$, $P = 0.03$ and $P < 0.001$, respectively). mRNA expression for MIP-2 (Fig. 9C) was significantly upregulated after LPS treatment at 100 ng/mL ($P = 0.02$) in BABL/c FasL$^{-/-}$ compared with WT mouse Mϕ but not at higher LPS concentrations or after PBS treatment. mRNA levels for IL-1β (Fig. 9D) were significantly upregulated in Mϕ from BALB/c FasL$^{-/-}$ over WT mice at LPS concentrations of 100 ng/mL and 10 μg/mL ($P = 0.03$ and $P = 0.02$, respectively) but not at other concentrations or after PBS. mRNA expression for IL-10 (Fig. 9E) was significantly downregulated in Mϕ from BALB/c FasL$^{-/-}$ compared with WT mice after LPS treatment at all concentrations except 100 ng/mL ($P = 0.03$, $P < 0.001$, and $P = 0.01$, respectively). No difference was found between the two groups after cells were treated with PBS. IL-12 mRNA expression (Fig. 9F) did not differ between the two groups at all LPS concentrations or after PBS.

DISCUSSION

Among numerous factors, apoptosis of cells appears an important regulatory mechanism contributing to disease modulation and resolution.[8,22,23] In fact, previous studies[5] have shown that

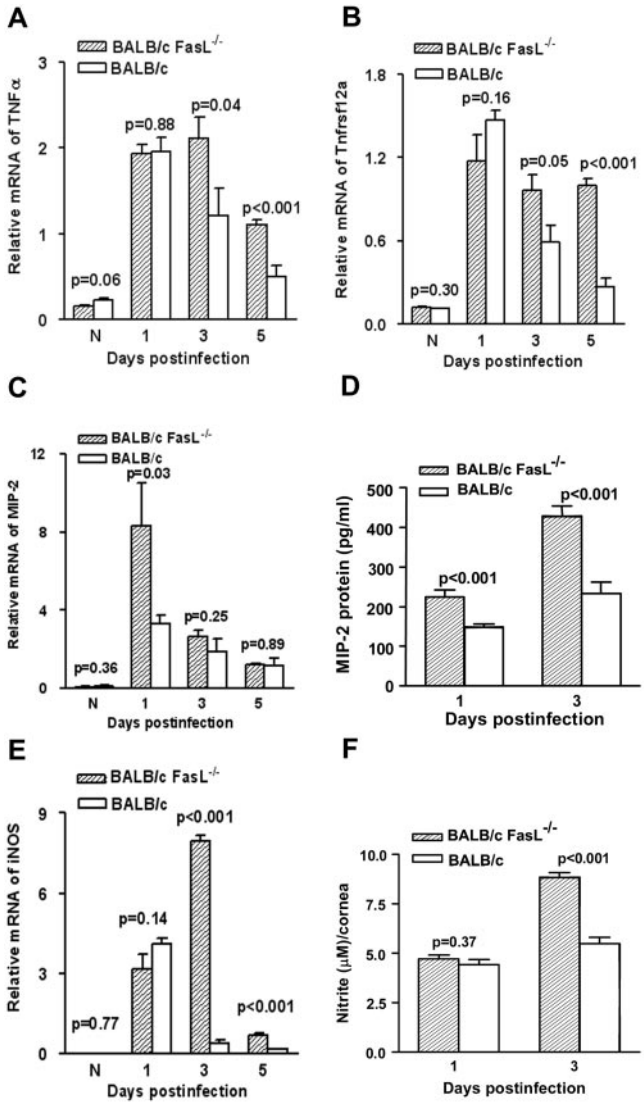

FIGURE 7. RT-PCR, ELISA and Griess reaction (n = 5/group/time/test). (**A**, **B**) Corneal mRNA expression for TNF-α (**A**) and its receptor (**B**) were upregulated in BALB/c FasL$^{-/-}$ compared with WT mice at 3 ($P = 0.04$; $P = 0.05$) and 5 ($P < 0.001$) days p.i. No differences were detected for either gene between groups at 1 day p.i. or in the normal, uninfected cornea. (**C**) MIP-2 mRNA expression was upregulated in BALB/c FasL$^{-/-}$ compared with WT mouse cornea at 1 day p.i. ($P = 0.03$) but not at 3 and 5 days p.i. No difference was detected in the normal, uninfected cornea between groups. (**D**) Corneal MIP-2 protein levels were higher in the cornea of BALB/c FasL$^{-/-}$ compared with WT mice at 1 day and 3 days p.i. ($P < 0.001$). (**E**) BALB/c FasL$^{-/-}$ compared with WT mice showed higher corneal mRNA levels of iNOS at 3 and 5 days p.i. ($P < 0.001$). No difference was detected at 1 day p.i. or in the normal, uninfected cornea between groups. (**F**) BALB/c FasL$^{-/-}$ compared with WT mice showed increased nitrite in the cornea at 3 days p.i. ($P < 0.001$). No difference was detected at 1 day p.i. between groups.

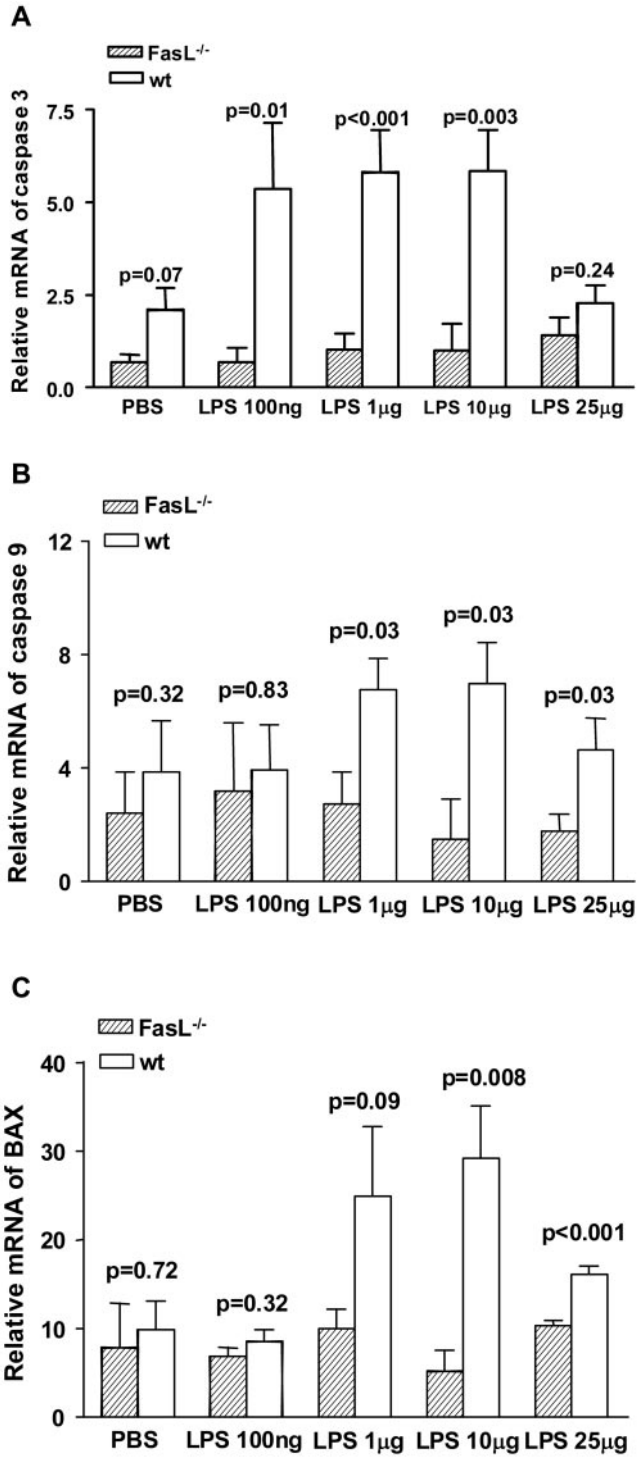

FIGURE 8. RT-PCR of apoptosis-related genes (n = 5/group/time/test). (**A**) Caspase mRNA expression was decreased in BALB/c FasL$^{-/-}$ compared with WT mice Mϕ after LPS treatment at all concentrations except 25 μg/mL (P = 0.01, $P < 0.001$, and P = 0.003, respectively). (**B**) Caspase 9 mRNA levels were lower in BALB/c FasL$^{-/-}$ than in WT Mϕ after LPS treatment at all tested concentrations except 100 ng/mL (P = 0.03 for all). (**C**) Mϕ from BALB/c FasL$^{-/-}$ mice expressed less BAX after LPS treatment at concentrations of 10 and 25 μg/mL compared with cells from WT mice (P = 0.008 and $P < 0.001$). No differences were detected at LPS concentrations of 100 ng/mL and 1 μg/mL between groups, and no differences were detected after PBS.

delay in PMN apoptosis correlated with poorer disease outcome (corneal perforation) in B6 mice. This effect could be reversed by treatment of these mice with Spantide I, which blocked the interaction of Substance P, an antiapoptotic neuropeptide, with its receptor and reduced activity. This resulted in earlier apoptosis and improved disease outcome.[5] Unfortunately, these data provided no evidence of involvement of a specific apoptotic pathway that might be used as a target for disease manipulation.

Apoptosis can be induced through the extrinsic death receptor or the intrinsic mitochondrial pathway; the former is subdivided into either the TNF or the Fas-FasL pathway.[6,7] In this regard, Alaoui-El-Azher et al.[9] reported that ExoS of *P. aeruginosa* triggered apoptosis by cleavage of caspase 8 in HeLa cells. This was inhibited by the overexpression of a dominant-negative version of the Fas-associated death domain, suggesting activation of the Fas pathway. Confocal laser scanning microscopy supported these data in that *P. aeruginosa* was shown to induce clustering of Fas. Consistently, another group induced rapid development of sepsis in Fas- or FasL-deficient, but not in WT, mice after *P. aeruginosa*-induced lung infection, indicating a protective role for Fas/FasL-mediated lung epithelial cell apoptosis.[8] In addition, FasL was critical in response to experimental *Staphylococcus aureus* endophthalmitis, and mice deficient in FasL were unable to control infection.[24] These studies are consistent with the study reported herein in which we show that signaling by the Fas pathway induces earlier apoptosis of inflammatory cells in WT BALB/c mice after *P. aeruginosa* corneal infection and that this is consistent with better disease prognosis. BALB/c FasL$^{-/-}$ mice, which bear a nonfunctional mutation in the *FasL^{gld}* gene, showed a pattern of delayed apoptosis (not seen until 3 days p.i.) and elevated caspase 3 and 9 levels at that time. These data support the hypothesis that other pathways of apoptosis are operative in the FasL$^{-/-}$ mouse cornea. However, the delayed apoptosis in BALB/c FasL$^{-/-}$ mice did not occur without adverse consequences and correlated with increased corneal bacterial counts and PMN infiltration. The latter may seem paradoxical but can be explained if one considers that with a delay in apoptosis, the persistence of PMN fuels stromal destruction (e.g., enzymes and cytokine release) and that this, in turn, provides a nutrient-rich "broth" that would favor bacterial growth and replication.

B6 FasL$^{-/-}$ compared with WT mice also were tested to exclude the possibility that genetic discrepancies in addition to FasL were involved. For example, it was reported[25] that the number of *Qa-2* genes, a member of the nonclassical major histocompatibility complex class Ib molecules, is variable in different mouse strains, with some strains expressing all four *Qa-2* genes (B6 mice), others expressing two (BALB/cJ mice), and still others being deleted for the Qa-2 locus (C3H/HeJ and BALB/cByJ mice). Our data suggested no role for the Qa-2 locus and indicated that mutation of the *FasL^{gld}* gene itself led to worsened disease outcome. In fact, we observed a delay in the onset of apoptosis and earlier corneal perforation in B6 FasL$^{-/-}$ mice. This group also had more (approximately fourfold) bacteria and PMN (MPO assay) in the cornea than did WT B6 mice, consistent with the pattern reported herein for BALB/c FasL$^{-/-}$ mice. In addition, we had to test the possibility that FasL/Fas-mediated apoptosis is not essential in regulating the lifespan of PMNs, as reported by others.[26] For this we used TUNEL staining and immunostaining. The data clearly show that the cells that undergo apoptosis in the BALB/c FasL$^{-/-}$ mouse cornea are PMNs, thus corroborating those findings and suggesting that in the absence of FasL, other pathways of apoptosis, though less timely, are activated and can regulate the PMN lifespan. TUNEL staining confirmed the delayed apoptotic pattern in knockout versus WT BALB/c mice, and RT-PCR combined with immunostaining correlated these data

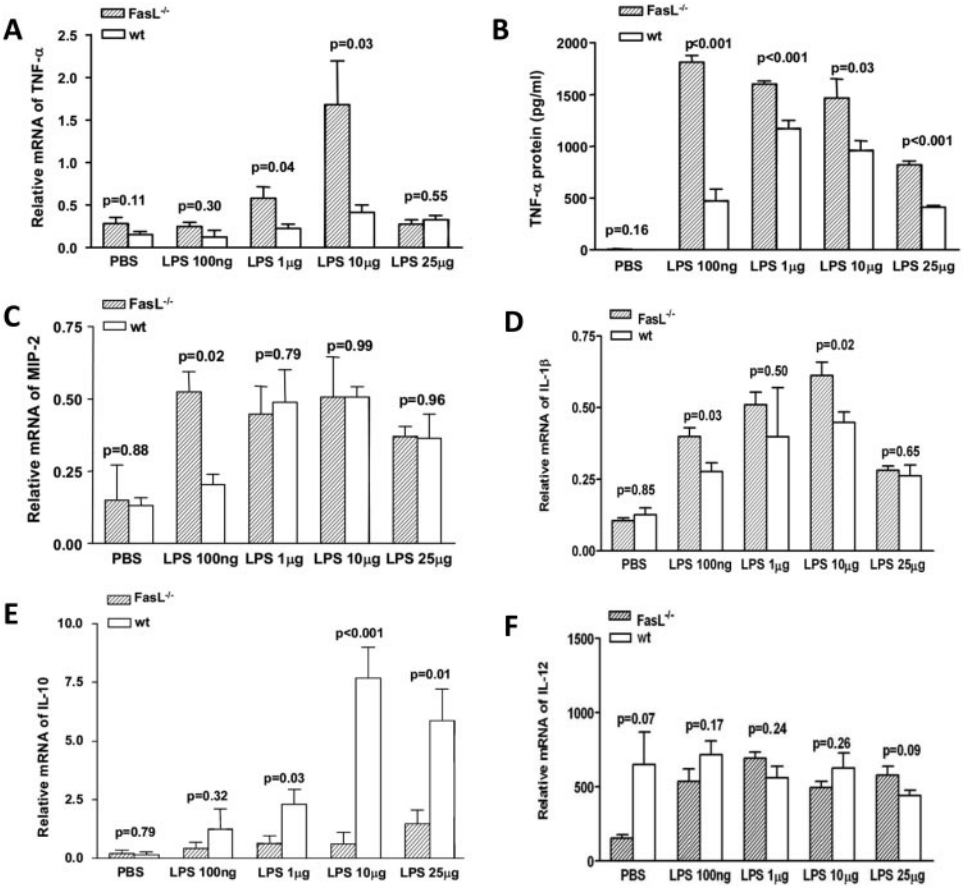

FIGURE 9. Real-time RT-PCR and ELISA for cytokine/chemokine expression (n = 5/group/time/test). (**A**) TNF-α mRNA expression was upregulated in BALB/c FasL$^{-/-}$ compared with WT Mϕ at LPS at concentrations of 1 and 10 μg/mL ($P = 0.04$ and $P = 0.03$, respectively). No differences were detected at other concentrations or after PBS treatment. (**B**) TNF-α protein levels were elevated in supernatants of BALB/c FasL$^{-/-}$ compared with WT Mϕ after LPS (all concentrations) but not after PBS ($P < 0.001$, $P < 0.001$, $P = 0.03$, and $P < 0.001$ respectively). (**C**) MIP-2 mRNA levels were elevated in BALB/c FasL$^{-/-}$ compared with WT Mϕ after LPS at 100 ng/mL ($P = 0.02$). No differences were detected at other concentrations or after PBS treatment. (**D**) mRNA expression for IL-1β was increased in Mϕ from BALB/c FasL$^{-/-}$ compared with WT mice after LPS treatment at 100 ng/mL and 10 μg/mL ($P = 0.03$ and $P = 0.02$, respectively) but not at other concentrations or after PBS. (**E**) IL-10 mRNA expression was decreased in LPS stimulated Mϕ from BALB/c FasL$^{-/-}$ compared with WT mice at all concentrations except 100 ng/mL ($P = 0.03$, $P < 0.001$, and $P = 0.01$ respectively). No difference was detected between the groups after PBS. (**F**) No difference was detected for IL-12 mRNA expression after LPS treatment (all tested concentrations) or after PBS in Mϕ from either group.

with caspase mRNA levels. The major initiator caspase in the Fas-FasL pathway, caspase 8,[6,7] which had not been tested before,[5] was downregulated in BALB/c FasL$^{-/-}$t versus WT mice after corneal infection. Knockout mice also showed delayed upregulation of both caspase 3 (BALB/c and B6 backgrounds) and caspase 9 (only BALB/c tested) compared with WT mice, and these data were similar to those shown when comparing susceptible B6 with resistant BALB/c mice.[5] Caspase 9 is mainly an initiator caspase related to the intrinsic pathway, which, on stress (e.g., infection), triggers mitochondrial release of cytochrome *c*, which binds to apoptotic protease-activating factor-1, or Apaf-1. The latter recruits and activates initiator caspase 9, leading to effector caspase stimulation and cell degradation.[27–29] The data suggest that when the Fas pathway is compromised (as in the knockout mouse), other pathways, such as the intrinsic pathway, may be activated and responsible for the induction of apoptosis when the Fas pathway is not functional, as in this study.

Bcl-2, BAX, Bcl-XL, and Bad, intracellular regulatory proteins, function either to inhibit or promote cell death, contributing to the maintenance of local tissue homeostasis.[30–32] In the present study, the gene expression patterns of proapoptotic BAX (upregulated early in WT mice but delayed in knockout mice) and antiapoptotic Bcl-2 (upregulated early in knockout and later in WT) were consistent with the observed pattern of delayed apoptosis in the infected corneas of FasL$^{-/-}$ mice, on either the BALB/c or the B6 background, suggesting that these intracellular molecules may contribute to or modulate Fas-mediated apoptosis.

Nonetheless, controversy exists concerning the outcome of Fas-FasL interaction in the regulation of inflammatory processes.[33] Data provided herein suggest an anti-inflammatory/protective role for Fas-FasL in the infected cornea in that we detected upregulated gene expression for TNF-α and its receptor (Tnfrsf12a), MIP-2, and enhanced PMN infiltration in FasL$^{-/-}$ compared with WT mouse cornea. In this regard, TNF-α may significantly improve PMN recruitment and is critical for prompt clearance of the bacteria,[34] but it also may be detrimental[35] if its proinflammatory effects are not balanced. Our data also are consistent with other reports that Fas activation can transmit stimulatory signals to certain cell types, including dendritic cells (DCs) and Mϕ, in inflamed synovial tissue after *B. burgdorferi* infection, resulting in enhanced cytokine production and worsened disease outcome.[10] In another study of *Pneumocystis pneumonia* infection,[36] Fas-FasL interaction resulted in the upregulation of IL-1β and TNF-α secretion by β-glucan–stimulated DCs and the dysregulation of FasL-enhanced exuberant and prolonged cytokine production, promoting lung inflammation.

In addition, we detected increased upregulation of gene expression for iNOS and its stable oxidized product, NO, in the infected BALB/c FasL$^{-/-}$ compared with WT mouse cornea. Despite a beneficial role in host defense, our data are consistent with the hypothesis that if NO is unregulated, serious pathologic conditions ensue not only in keratitis but also in other diseases such as septic shock and respiratory distress syndrome.[37]

Mϕ release an array of mediators, including proinflammatory cytokines such as TNF-α, IL-12, IL-1, and IL-6 and anti-inflammatory cytokines such as IL-10 and TGF-β.[38] Studies have shown that Fas-FasL interaction regulates inflammatory reactions by triggering the apoptosis of Mϕ and modulating cytokine/chemokine secretion patterns.[39–41] In the in vitro study reported herein, we show downregulated expression for proapoptotic genes, including caspases 3 and 9 and BAX, and upregulated proinflammatory cytokines/chemokines MIP-2, IL-1β, and TNF-α in LPS-stimulated Mϕ from FasL$^{-/-}$ compared with WT mice. These data are consistent with our in vivo data

and provide further confirmation of a Fas pathway proapoptotic and protective role in this disease model. We also detected downregulation of the anti-inflammatory cytokine IL-10 in Mϕ from FasL$^{-/-}$ mice, whereas mRNA expression for IL-12 (proinflammatory) showed no difference between the two groups. These data suggest that lower levels of IL-10 in cells from knockout mice would theoretically be less able to balance IL-12 levels than WT mice. In this regard, previous work from this laboratory[5] showed that IL-10 was upregulated in Mϕ from BALB/c compared with B6 mice and that, after subconjunctival injection of clodronate-containing liposomes to deplete Mϕ in BALB/c mice, higher levels of IFN-γ and lower levels of IL-10 were detected, and these normally resistant mice were converted to the susceptible phenotype.[21]

In conclusion, this study has shown that in the absence of Fas-FasL interaction from the knockout of FasL, apoptosis is delayed, PMNs persist longer in the stroma, and local production of proinflammatory cytokines/chemokines and NO is enhanced compared with the response of WT mice. A delay of this early innate immune apoptotic response in the cornea subsequently leads to worsened disease outcome and corneal destruction. In vitro, signaling by the Fas pathway appears necessary for the upregulation of Mϕ apoptosis-related genes, the downregulation of proinflammatory cytokine/chemokine expression, and the upregulation of sufficient amounts of IL-10 to balance IL-12 gene expression.

References

1. Hazlett LD. Corneal response to *Pseudomonas aeruginosa* infection. *Prog Retin Eye Res.* 2004;23:1–30.
2. Mondino BJ, Weissman BA, Farb MD, Pettit TH. Corneal ulcers associated with daily-wear and extended-wear contact lenses. *Am J Ophthalmol.* 1986;102:58–65.
3. Rattanatam TW, Heng WJ, Rapuano CJ, Laibson RR, Cohen EJ. Trends in contact lens-related corneal ulcers. *Cornea.* 2001;20:290–294.
4. Szliter EA, Lighvani S, Barrett RP, Hazlett LD. Vasoactive intestinal peptide balances pro- and anti-inflammatory cytokines in the *Pseudomonas aeruginosa*-infected cornea and protects against corneal perforation. *J Immunol.* 2007;178:1105–1114.
5. Zhou Z, Barrett RP, McClellan SA, et al. Substance P delays apoptosis, enhancing keratitis after *Pseudomonas aeruginosa* infection. *Invest Ophthalmol Vis Sci.* 2008;49:4458–4467.
6. Steller H. Mechanisms and genes of cellular suicide. *Science.* 1995;267:1445–1449.
7. Tibbetts MD, Zheng L, Lenardo MJ. The death effector domain protein family: regulators of cellular homeostasis. *Nat Immunol.* 2003;4:404–409.
8. Grassme H, Kirschnek S, Riethmueller J, et al. CD95/CD95 ligand interactions on epithelial cells in host defense to *Pseudomonas aeruginosa*. *Science.* 2000;20:527–530.
9. Alaoui-El-Azher M, Jia J, Lian W, Jin S. ExoS of *Pseudomonas aeruginosa* induces apoptosis through a Fas receptor/caspase 8-independent pathway in HeLa cells. *Cell Microbiol.* 2006;8:326–338.
10. Shi C, Wolfe J, Russell JQ, et al. Fas ligand deficiency impairs host inflammatory response against infection with the spirochete Borrelia burgdorferi. *Infect Immun.* 2006;74:1156–60.
11. Hazlett LD, Moon MM, Strejc M, Berk RS. Evidence for N-acetylmannosamine as an ocular receptor for *P. aeruginosa* adherence to scarified cornea. *Invest Ophthalmol Vis Sci.* 1987;28:1978–1985.
12. Kernacki KA, Barrett RP, Hobden JA, Hazlett LD. Macrophage inflammatory protein-2 is a mediator of polymorphonuclear neutrophil influx in ocular bacterial infection. *J Immunol.* 2000;164:1037–1045.
13. McClellan SA, Zhang Y, Barrett RP, Hazlett LD. Substance P promotes susceptibility to *Pseudomonas aeruginosa* keratitis in resistant mice: anti-inflammatory mediators downregulated. *Invest Ophthalmol Vis Sci.* 2008;49:1502–1511.
14. Hazlett LD, McClellan SA, Barrett RP, Liu J, Zhang Y, Lighvani S. Spantide I decreases type I cytokines, enhances IL-10, and reduces corneal perforation in susceptible mice after *Pseudomonas aeruginosa* infection. *Invest Ophthalmol Vis Sci.* 2007;48:797–807.
15. Huang X, Du W, Barrett RP, Hazlett LD. ST2 is essential for Th2 responsiveness and resistance to *Pseudomonas aeruginosa* keratitis. *Invest Ophthalmol Vis Sci.* 2007;48:4626–4633.
16. Kernacki KA, Goebel DJ, Poosch MS, LD. Hazlett. Early cytokine and chemokine gene expression during *Pseudomonas aeruginosa* corneal infection in mice. *Infect Immun.* 1998;66:376–379.
17. Williams RN, Paterson CA. PMN accumulation in aqueous humor and iris-ciliary body during intraocular inflammation. *Invest Ophthalmol Vis Sci.* 1984;25:105–108.
18. Williams RN, Paterson CA, Eakins KE, Bhattacherjee P. Quantification of ocular inflammation: evaluation of polymorphonuclear leucocyte infiltration by measuring myeloperoxidase activity. *Curr Eye Res.* 1982;2:465–470.
19. McClellan SA, Lighvani S, Hazlett LD. IFN-gamma: regulation of nitric oxide in the *P. aeruginosa*-infected cornea. *Ocul Immunol Inflamm.* 2006;14:21–28.
20. Zhang Y, Gabriel MM, Mowrey-McKee MF, Barrett RP, McClellan S, Hazlett LD. Rat silicone hydrogel contact lens model: effects of high- versus low-Dk lens wear. *Eye Contact Lens.* 2008;34:306–311.
21. McClellan SA, Huang X, Barrett RP, van Rooijen N, Hazlett LD. Macrophages restrict *Pseudomonas aeruginosa* growth, regulate polymorphonuclear neutrophil influx, and balance pro- and anti-inflammatory cytokines in BALB/c mice. *J Immunol.* 2003;170:5219–5227.
22. Allenbach C, Zufferey C, Perez C, Launois P, Mueller C, Tacchini-Cottier F. Macrophages induce neutrophil apoptosis through membrane TNF, a process amplified by *Leishmania major*. *J Immunol.* 2006;11:6656–6664.
23. Bockmann S, Seep J, Jonas L. Delay of neutrophil apoptosis by the neuropeptide substance P: involvement of caspase cascade. *Peptides.* 2001;22:661–670.
24. Engelbert M, Gilmore MS. Fas ligand but not complement is critical for control of experimental *Staphylococcus aureus* endophthalmitis. *Invest Ophthalmol Vis Sci.* 2005;46:2479–2486.
25. Niederkorn JY, Chiang EY, Ungchusri T, Stroynowski I. Expression of a nonclassical MHC class Ib molecule in the eye. *Transplantation.* 1999;68:1790–1799.
26. Fecho K, Cohen PL. Fas ligand (gld)- and Fas (lpr)-deficient mice do not show alterations in the extravasation or apoptosis of inflammatory neutrophils. *J Leukoc Biol.* 1998;64:373–383.
27. Li P, Nijhawan D, Budihardjo I, et al. Cytochrome *c* and dATP-dependent formation of Apaf-1/caspase-9 complex initiates an apoptotic protease cascade. *Cell.* 1997;91:479–489.
28. Liu X, Kim CN, Yang J, Jemmerson R, Wang X. Induction of apoptotic program in cell-free extracts: requirement for dATP and cytochrome *c*. *Cell.* 1996;86:147–157.
29. Zou H, Henzel WJ, Liu X, Lutschg A, Wang X. Apaf-1, a human protein homologous to C. elegans CED-4, participates in cytochrome c-dependent activation of caspase-3. *Cell.* 1997;90:405–413.
30. Hengartner MO, Ellis RE, Horvitz HR. *Caenorhabditis elegans* gene ced-9 protects cells from programmed cell death. *Nature.* 1992;356:494–499.
31. Korsmeyer SJ. Bcl-2 initiates a new category of oncogenes: regulators of cell death. *Blood.* 1992;80:879–886.
32. Vaux DL, Weissman IL, Kim SK. Prevention of programmed cell death in *Caenorhabditis elegans* by human Bcl-2. *Science.* 1992;258:1955–1957.
33. Gregory MS, Saff RR, Marshak-Rothstein A, Ksander BR. Control of ocular tumor growth and metastatic spread by soluble and membrane Fas ligand. *Cancer Res.* 2007;67:11951–11958.
34. Morisette C, Francoeur C, Darmond-Zwaig C, Gervais F. Lung phagocyte bactericidal function in strains of mice resistant and susceptible to *Pseudomonas aeruginosa*. *Infect Immun.* 1996;64:4984–4992.

35. Hazlett LD, Rudner XL, McClellan SA, Barrett RP, Lighvani S. Role of IL-12 and IFN-gamma in *Pseudomonas aeruginosa* corneal infection. *Invest Ophthalmol Vis Sci.* 2002;43:419–424.
36. Carmona EM, Vassallo R, Vuk-Pavlovic Z, Standing JE, Kottom TJ, Limper AH. Pneumocystis cell wall beta-glucans induce dendritic cell costimulatory molecule expression and inflammatory activation through a Fas-Fas ligand mechanism. *J Immunol.* 2006;177:459–467.
37. Delgado M, Martinez C, Pozo D, et al. Vasoactive intestinal peptide (VIP) and pituitary adenylate cyclase-activation polypeptide (PACAP) protect mice from lethal endotoxemia through the inhibition of TNF-α and IL-6. *J Immunol.* 1999;162:1200–1205.
38. Laskin DL, Pendino KJ. Macrophages and inflammatory mediators in tissue injury. *Annu Rev Pharmacol Toxicol.* 1995;35:655–677.
39. O'Connell J. Immune privilege or inflammation? The paradoxical effects of Fas ligand. *Arch Immunol Ther Exp (Warsz).* 2000;48:73–79.
40. Altemeier WA, Zhu X, Berrington WR, Harlan JM, Liles WC. Fas (CD95) induces macrophage proinflammatory chemokine production via a MyD88-dependent, caspase-independent pathway. *J Leukoc Biol.* 2007;82:721–728.
41. Chung CS, Song GY, Lomas J, Simms HH, Chaudry IH, Ayala A. Inhibition of Fas/Fas ligand signaling improves septic survival: differential effects on macrophage apoptotic and functional capacity. *J Leukoc Biol.* 2003;74:344–351.